Direct Writing of Metal Nanoparticle Films Inside Sealed Microfluidic Channels

ARTICLE *in* ANALYTICAL CHEMISTRY · FEBRUARY 2006

Impact Factor: 5.64 · DOI: 10.1021/ac051288j · Source: PubMed

4 AUTHORS, INCLUDING:

Sho Kataoka
National Institute of Advanced Industrial Sci…

50 PUBLICATIONS **1,295** CITATIONS

SEE PROFILE

Anal. Chem. **2006,** *78,* 107−112

Direct Writing of Metal Nanoparticle Films Inside Sealed Microfluidic Channels

Edward T. Castellana, Sho Kataoka, Fernando Albertorio, and Paul S. Cremer*

Department of Chemistry, Texas A&M University, College Station, Texas 77843

Herein we demonstrate the ability to pattern Ag nanoparticle films of arbitrary geometry inside sealed PDMS/TiO_2/glass microfluidic devices. The technique can be employed with aqueous solutions at room temperature under mild conditions. A 6 nm TiO_2 film is first deposited onto a planar Pyrex or silica substrate, which is subsequently bonded to a PDMS mold. UV light is then exposed through the device to reduce Ag^+ from an aqueous solution to create a monolayer-thick film of Ag nanoparticles. We demonstrate that this on-chip deposition method can be exploited in a parallel fashion to synthesize nanoparticles of varying size by independently controlling the solution conditions in each microchannel in which the film is formed. The film morphology was checked by atomic force microscopy, and the results showed that the size of the nanoparticles was sensitive to solution pH. Additionally, we illustrate the ability to biofunctionalize these films with ligands for protein capture. The results indicated that this could be done with good discrimination between addressed locations and background. The technique appears to be quite general, and films of Pd, Cu, and Au could also be patterned.

Chemically patterned surfaces within the confines of microfluidic channels enhance the flexibility and utility of lab-on-a-chip platforms.[1−4] For complex systems, significant attention has been focused on aligning prepatterned substrates with separately molded microchannels.[5−8] However, devising simple methods for controlling the surface chemistry inside microfluidic channels after device assembly could greatly enhance rapid prototyping capabilities. In fact, precise spatial control over the molecules presented on the channel walls avoids the need to bring prepatterned substrates into registry and allows materials to be utilized that cannot easily withstand harsh bonding procedures. Such issues can be critical in the design of microfluidic-based sensors, diagnostic devices, and microreactors. Until now, patterning inside sealed microfluidic devices has been quite challenging. This is especially true if one is interested in deposition methods involving aqueous solutions and mild conditions. There have been some strategies developed for organic and biological materials,[9] but procedures for addressing metals are particularly limited.[10]

Typically, metal patterning of substrates is carried out via top down methods beginning with the evaporation or sputtering of metal onto a substrate. This step is followed by either spin coating and lithographic patterning of photoresist or microcontact printing of thiol polymer multilayers.[11] Both procedures provide a protective masking layer during chemical etching of the unwanted regions of the deposited metal. Such procedures work extremely well for patterning planar substrates but would be extremely challenging to carry out inside enclosed poly(dimethylsiloxane) (PDMS) and glass microfluidic systems because of the impracticality of sputtering, stamping, or spin coating materials inside enclosed architectures. Another approach has been to photoreduce metals from polymer solutions and films onto planar substrates.[12,13] Unfortunately, such methods would be cumbersome to employ in microchannel networks as the macromolecular catalysts for metal reduction would be hard to remove after the metal is deposited.

Currently, the most practical strategy available for patterning metals inside sealed microchannels involves the use of multiphase laminar flow.[10] Similar techniques have also been exploited for the patterning of polymers,[14] inorganic crystals, proteins, and cells.[15] These methods, however, produce architectures that are limited by the flow profiles generated within specific channel geometries and often must be formed downstream from a channel junction. We therefore aimed to devise a simple procedure that would allow metal films to be patterned inside sealed microfluidic systems from an aqueous solution under mild conditions with almost any design.

* To whom correspondence should be addressed. E-mail: cremer@mail.chem.tamu.edu.

(1) Yang, T. L.; Jung, S. Y.; Mao, H. B.; Cremer, P. S. *Anal. Chem.* **2001**, *73*, 165−169.
(2) Caelen, I.; Bernard, A.; Juncker, D.; Michel, B.; Heinzelmann, H.; Delamarche, E. *Langmuir* **2000**, *16*, 9125−9130.
(3) Barker, S. L. R.; Tarlov, M. J.; Canavan, H.; Hickman, J. J.; Locascio, L. E. *Anal. Chem.* **2000**, *72*, 4899−4903.
(4) Delamarche, E.; Bernard, A.; Schmid, H.; Bietsch, A.; Michel, B.; Biebuyck, H. *J. Am. Chem. Soc.* **1998**, *120*, 500−508.
(5) Su, J.; Bringer, M. R.; Ismagilov, R. F.; Mrksich, M. *J. Am. Chem. Soc.* **2005**, *127*, 7280−7281.
(6) Cesaro-Tadic, S.; Dernick, G.; Juncker, D.; Buurman, G.; Kropshofer, H.; Michel, B.; Fattinger, C.; Delamarche, E. *Lab Chip* **2004**, *4*, 563−569.
(7) Khademhosseini, A.; Suh, K. Y.; Jon, S.; Eng, G.; Yeh, J.; Chen, G. J.; Langer, R. *Anal. Chem.* **2004**, *76*, 3675−3681.
(8) Jiang, X. Y.; Ng, J. M. K.; Stroock, A. D.; Dertinger, S. K. W.; Whitesides, G. M. *J. Am. Chem. Soc.* **2003**, *125*, 5294−5295.
(9) Holden, M. A.; Jung, S. Y.; Cremer, P. S. *Anal. Chem.* **2004**, *76*, 1838−1843.
(10) Kenis, P. J. A.; Ismagilov, R. F.; Whitesides, G. M. *Science* **1999**, *285*, 83−85.
(11) Huck, W. T. S.; Yan, L.; Stroock, A.; Haag, R.; Whitesides, G. M. *Langmuir* **1999**, *15*, 6862−6867.
(12) Korchev, A. S.; Bozack, M. J.; Slaten, B. L.; Mills, G. *J. Am. Chem. Soc.* **2004**, *126*, 10−11.
(13) Baldacchini, T.; Pons, A. C.; Pons, J.; LaFratta, C. N.; Fourkas, J. T.; Sun, Y.; Naughton, M. J. *Opt. Express* **2005**, *13*, 1275−1280.
(14) Li, S. L.; Macosko, C. W.; White, H. S. *Science* **1993**, *259*, 957−960.
(15) Takayama, S.; McDonald, J. C.; Ostuni, E.; Liang, M. N.; Kenis, P. J. A.; Ismagilov, R. F.; Whitesides, G. M. *Proc. Natl. Acad. Sci. U.S.A.* **1999**, *96*, 5545−5548.

10.1021/ac051288j CCC: $33.50
Published on Web 11/18/2005

TiO_2 is a well-known photocatalyst for water and air purification.[16] UV illumination produces electrons and holes that can be used to oxidize and reduce a wide range of organic and inorganic species on its surface, including metal ions from aqueous solutions. In particular, photocatalytic deposition of Ag into a sol–gel-derived TiO_2 matrix and onto TiO_2 particles has been shown to occur from Ag^+ in aqueous solution.[17–21] Adsorbed Ag^+ ions are reduced by the photogenerated electrons, and water undergoes oxidative decomposition by the holes.[22] This process typically generates metal nanoparticles, where the particles vary in size and shape depending upon the exact conditions employed.[23] Such methods have been extended to patterning metals onto TiO_2 nanoparticles at interfaces[24] and should even be useful for patterning inside microfluidic channels if a thin TiO_2 coating on a planar support were used instead of the nanoparticles. Indeed, we reasoned that this would be possible as long as the distance the electron/hole pair diffused from the initial site of excitation was fairly restricted. The utility of the technique lies in the fact that the surface of the microchannel itself would now be the catalyst for metal deposition. Such a technique is compatible with aqueous solutions and ambient conditions, which is ideal for microchannel surface modification.

Our strategy for patterning Ag nanoparticle films involves the reduction of Ag^+ from an aqueous $AgNO_3$ solution by selectively illuminating the desired areas of the microchannel with UV radiation through a photomask. After a metal film has been deposited, its surface can be further tailored by employing thiol chemistry. In fact, we found that the serial introduction of metal patterns at specific locations, followed by surface derivatization easily led to the presentation of spatially addressed biosensor architectures (Figure 1). Moreover, several different metals including Pd could be patterned in addition to silver.

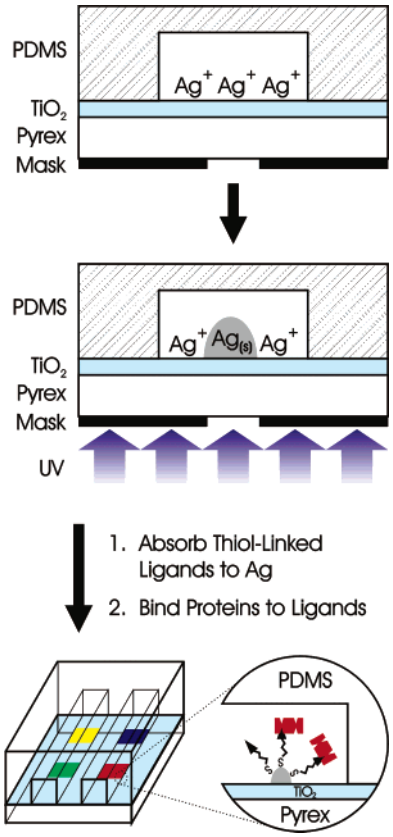

Figure 1. Schematic diagram for the deposition of a silver nanoparticle film. First, a $AgNO_3$ solution is introduced into the microchannel. Next, UV radiation is passed through a photomask onto the backside of the TiO_2 thin film. Ag^+ ions adsorbed at the interface are selectively reduced by photoelectrons, which grow into nanoparticle films. This process can be used in combination with thiol chemistry inside sealed microfluidic channels to address surface chemistries in almost any desired location or pattern.

EXPERIMENTAL SECTION

Materials. Polished Pyrex 7740 wafers (25.4 mm^2, 0.5 mm thick) were supplied by Precision Glass and Optics (Santa Ana, CA). Fused-silica coverslips (25 mm^2, 0.17 mm thick) were purchased from Structure Probe, Inc. (West Chester, PA). Biotin PEG disulfide (structure 1),

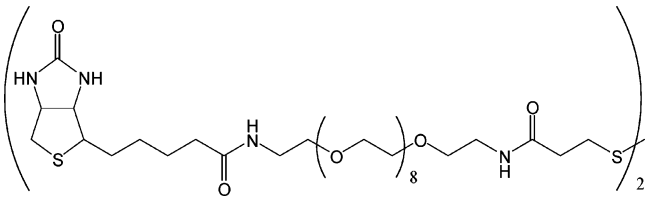

and PEG propionate disulfide (structure 2)

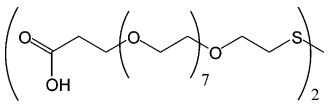

were obtained from BioVectra Inc (Prince Edward Island, Canada). *N*-(2,4-Dinitrophenyl)cadaverine hydrochloride (DNP-cadaverine) was acquired from Axxora (San Diego, CA). Streptavidin Alexa Fluor 594 conjugate (Strep-A594), anti-dinitrophenyl-KLH, rabbit IgG fraction Alexa Fluor 488 conjugate (anti-DNP-A488) were supplied by Invitrogen (Eugene, OR). Poly(dimethylsiloxane) (Dow Corning Sylgard Silicone Elastomer-184) was obtained from Krayden, Inc (El Paso, TX). Silver nitrate, palladium chloride, *N*-ethyl-*N*′-(3-dimethylaminopropyl)carbodiimide hydrochloride (EDC), sodium phosphate, 4-(2-hydroxyethyl)piperazine-1-ethanesulfonic acid (HEPES buffer salt), and sodium chloride were purchased from Sigma-Aldrich (St. Louis, MO). These materials were used as provided.

TiO_2 Film Preparation. Smooth films of TiO_2 were prepared using our previously established room temperature and pressure

(16) Hoffmann, M. R.; Martin, S. T.; Choi, W. Y.; Bahnemann, D. W. *Chem. Rev.* **1995**, *95*, 69–96.
(17) Shchukin, D.; Ustinovich, E.; Sviridov, D.; Pichat, P. *Photochem. Photobiol.* **2004**, *3*, 142–144.
(18) Szabo-Bardos, E.; Czili, H.; Horvath, A. *J. Photochem. Photobiol., A* **2003**, *154*, 195–201.
(19) Sahyun, M. R. V.; Serpone, N. *Langmuir* **1997**, *13*, 5082–5088.
(20) Fleischauer, P. D.; Shepherd, J. R.; Kan, H. K. A. *J. Am. Chem. Soc.* **1972**, *94*, 283-&.
(21) Litter, M. I. *Appl. Catal., B* **1999**, *23*, 89–114.
(22) Nishimoto, S.; Ohtani, B.; Kajiwara, H.; Kagiya, T. *J. Chem. Soc., Faraday Trans. 1* **1983**, *79*, 2685–2694.
(23) Zhang, F. X.; Guan, N. J.; Li, Y. Z.; Zhang, X.; Chen, J. X.; Zeng, H. S. *Langmuir* **2003**, *19*, 8230–8234.
(24) Ikeda, S.; Akamatsu, K.; Nawafune, H. *J. Mater. Chem.* **2001**, *11*, 2919–2921.

chemical vapor deposition protocol.[25] The film is grown via hydrolysis of titanium(IV) isopropoxide by OH groups on the substrate surface aided by small amounts of water vapor.[26,27] This process occurs inside the reaction chamber producing 2-propanol and TiO_2. Briefly, Pyrex 7740 wafers or silica coverslips were cleaned in piranha solution (1:3 ratio of 30% H_2O_2 and H_2SO_4. *Note: piranha is a vigorous oxidant and should only be used with extreme caution*) for 45 min, rinsed extensively with purified water (18.2 MΩ/cm^2, NANOpure Ultrapure Water System, Barnstead, Dubuque, IA), dried with nitrogen, and baked at 500 °C for 5 h. The wafers were then soaked in concentrated H_2SO_4 for 6 h, rinsed extensively with more purified water, rinsed with methanol, dried with nitrogen, and exposed to titanium(IV) isopropoxide vapor at room temperature for 2 h. The surface reaction was stopped by rinsing with purified water and reagent grade acetone. Finally, the slides were baked again at 500 °C for 5 h to facilitate calcination of the film. The thickness of the titania layer was measured to be 6 nm by ellipsometry (model L2W26D; Gaertner Scientific, Skokie, IL), using a 632-nm laser at 80° and assuming the index of refraction of the film was 2.46.[28,29]

Microfluidic Device Fabrication. PDMS microfluidic devices were fabricated using previously published soft lithography techniques.[1] The microfluidic devices consisted of five 300 μm wide by 8 μm deep channels. The PDMS and TiO_2/glass surfaces were treated with an oxygen plasma for 10−15 s and immediately brought into contact with each other to create a bond.[30] This formed channels with PDMS walls and a TiO_2 floor.

Synthesis of *N*-(2,4-Dinitrophenyl) PEG Disulfide. In 100 mL of HEPES buffer (10 mM HEPES, pH 7.4), 1 equiv of PEG propionate disulfide (2 mM) was reacted with 2 equiv of DNP-cadaverine in the presence of 3 equiv of EDC. The EDC coupling reaction was allowed to proceed for 24 h at room temperature in the dark under constant agitation. The formation of *N*-(2,4-dinitrophenyl) PEG disulfide (DNP-PEG-disulfide) was confirmed by matrix-assisted laser desorption/ionization (MALDI) mass spectrometry. The structure of DNP-PEG-disulfide is shown as structure 3.

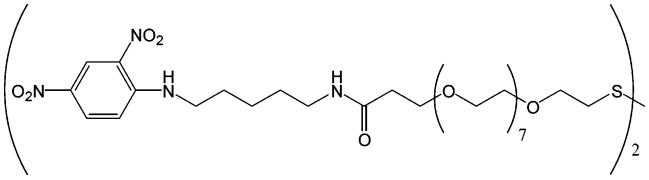

Direct Writing of Silver Films. Thin silica cover slips (0.17 mm) coated with TiO_2 films were used for higher resolution Ag patterns, and thicker (0. 5 mm) Pyrex supports were used in all other cases. UV patterning of Ag films was performed with a mask aligner (Quintel Q400MA, San Jose, CA) through a high-resolution test mask (Edmund Industry Optics, Barrington, NJ). The patterned Ag films were imaged using bright-field illumination on a Nikon Eclipse 80i fluorescence microscope with a Princeton Instruments 1024B MicroMax CCD camera (Trenton, NJ). The same instrument was used for fluorescence imaging. Individual false color images of the fluorescence from the bound strep-A594 and anti-DNP-A488 in the sealed microchannels were combined in Adobe Photoshop 5.0. For Ag patterning experiments performed as a function of pH, the pH value of the silver solutions was adjusted with appropriate amounts of HNO_3 or NaOH. AFM imaging was performed with a Nanoscope IIIa (Digital Instruments, Santa Barbara, CA) equipped with a J-type scanner and silicon cantilever tips (Mikro Masch, Wilsonville, OR).

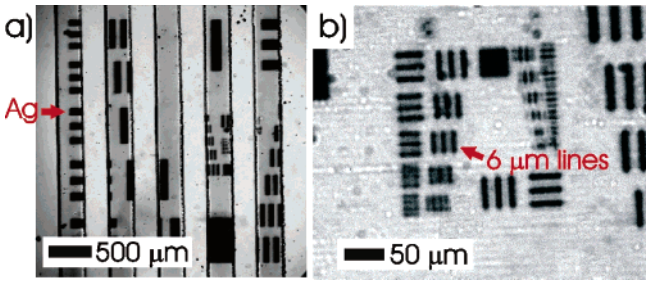

Figure 2. (a) Bright-field image, 4×, of silver nanoparticles patterned inside sealed microfluidic channels by lithographic photocatalytic deposition. Each channel has a width of 300 μm. (b) Bright-field image under a 40× objective pointing out 6-μm-wide lines.

RESULTS

Direct Writing of Silver Films. In a first set of experiments, a solution of 0.1 M $AgNO_3$ at pH 5.0 was injected into a series of five parallel microfluidic channels. The channels consisted of PDMS walls and a TiO_2 floor. UV light (11 mW/cm^2 near 365 nm) was used to selectively illuminate different regions of the TiO_2 surface through a chrome test mask for 20 min. This resulted in the direct writing of silver by photocatalytic reduction inside the microchannels as could be verified by bright-field imaging of the device (Figure 2a). The chemical composition of the film was verified by XPS (Kratos Axis Ultra Imaging X-ray photoelectron spectrometer, Manchester, U.K.). As can be seen, the film could be patterned with nearly any geometry desired and the feature resolution was ~10 μm.

Next, we wanted to verify that Ag nanoparticle films could be patterned with at least micrometer-scale resolution. This required the use of a thinner support beneath the TiO_2-coated surface as UV light for patterning is introduced through the back of the substrate (Figure 1). To minimize feature distortion due to imperfect illumination conditions, a 0.17 mm silica slide was used as the support. This thinner support was chosen because light from a less than perfectly collimated source will lead to increasingly poorer image resolution the further the mask is offset from the TiO_2 film. The reason for employing silica rather than Pyrex stemmed from the fact that thinner silica substrates were more readily available from commercial sources. The results showed that patterns could easily be made with resolution down to a few micrometers (Figure 2b). For example, the red arrow points to a series of 6-μm-wide lines separated from one another by 6-μm spaces. The ultimate resolution of the mass aligner employed is ~2 μm. It should be noted that control experiments were

(25) Kataoka, S.; Gurau, M. C.; Albertorio, F.; Holden, M. A.; Lim, S. M.; Yang, R. D.; Cremer, P. S. *Langmuir* **2004**, *20*, 1662−1666.
(26) Fadeev, A. Y.; McCarthy, T. J. *J. Am. Chem. Soc.* **1999**, *121*, 12184−12185.
(27) Fadeev, A. Y.; McCarthy, T. J. *Langmuir* **1999**, *15*, 3759−3766.
(28) Remillard, J. T.; McBride, J. R.; Nietering, K. E.; Drews, A. R.; Zhang, X. *J. Phys. Chem. B* **2000**, *104*, 4440−4447.
(29) Alvarez-Herrero, A.; Fort, A. J.; Guerrero, H.; Bernabeu, E. *Thin Solid Films* **1999**, *349*, 212−219.
(30) To the best of our knowledge, this is the first report of irreversible bonding between PDMS and TiO_2 thin films.

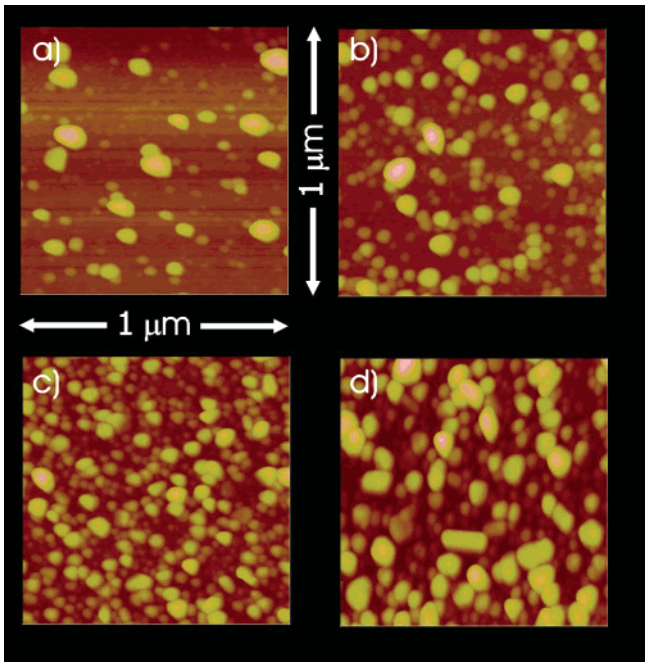

Figure 3. Tapping mode AFM images of Ag nanoparticle films deposited at (a) pH 2, (b) pH 3, (c) pH 5, and (d) pH 6.

performed with thicker silica substrates. The results demonstrated that patterning Ag films on TiO_2/silica behaved similarly to TiO_2/Pyrex under conditions of identical substrate thickness (data not shown).

Controlling Film Morphology at the Nanoscale. The ability to deposit Ag films inside microfluidic channels opens the door to on-chip studies of film morphology as a function of deposition conditions. To demonstrate this, experiments were performed as a function of the pH of the $AgNO_3$ solution. It is known that the pH of Ag^+ solutions affects the rate of silver deposition as well as the initial amount of Ag^+ adsorbed onto a TiO_2 surface.[31] This is caused in large part by the modulation in surface charge of the TiO_2 substrate as the pH is changed. We therefore reasoned that particle size might vary as the deposition pH is changed over the planar substrate. The deposition conditions were otherwise similar to those used in Figure 2. However, to enable investigation of nanoparticle size by AFM, the $AgNO_3$ solutions were injected into PDMS microchannels that were only pressed against the TiO_2 surface rather than plasma bonded with it. This allowed the PDMS mold to be pealed away from the substrate just prior to investigation by AFM. The substrate was rinsed with purified water and blown dry with N_2 gas before imaging in air. Deposition was undertaken at pH 2, 3, 5, and 6, and AFM images of the surface under the various conditions are shown in Figure 3.

The AFM results show that the mean particle size was 65 nm at pH 2, and image analysis revealed that the 1σ particle size distribution was 24 nm (Figure 3a). Under these conditions, the surface is positively charged, hence, limiting the rate of Ag^+ adsorption. This should lead to sparse nucleation sites and larger particles. As the pH is raised, the coverage becomes higher for fixed deposition time (20 min) and the mean nanoparticle size begins to decrease (Figure 3b and c). In these cases, the particle sizes were 62 nm with $1\sigma = 16$ nm at pH 3 and 51 nm with $1\sigma = 16$ nm at pH 5. Above the isoelectric point of the TiO_2 film (pI $\cong$ 5.5), the size again increases as does the relative surface coverage (mean particle size of 75 nm with $1\sigma = 26$ nm at pH 6). These results clearly demonstrate that at least limited control over nanoparticle size and coverage can be obtained through modulation of the bulk solution pH.

(31) Ohtani, B.; Okugawa, Y.; Nishimoto, S.; Kagiya, T. *J. Phys. Chem.* **1987**, *91*, 3550−3555.

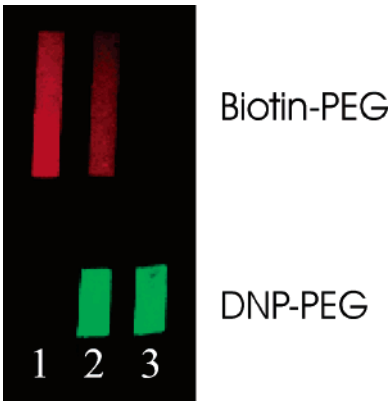

Figure 4. Fluorescence micrograph of fluorescently labeled proteins binding to derivatized silver nanoparticles. Channel 1 was injected only with streptavidin (red) and shows evidence of it binding almost exclusively to the biotin-derivatized nanoparticles, while the rest of the channel remains dark. Channel 3 was injected with anti-DNP (green), which is observed to bind only to the DNP-derivatized nanoparticles. Channel 2 was injected with both proteins, and hence, both binding events occurred.

Sensor Chip. To demonstrate the versatility of this technique for sensor design and biofunctionalization within sealed microchannels, a simple two-color fluorescence assay was developed wherein two separate ligands were patterned at different locations within a linear array of microfluidic channels. First, a strip of silver was patterned across three sealed microfluidic channels using the procedures described above. The channels were rinsed with purified water, filled with a solution of 2 mg/mL biotin PEG disulfide and 10 mg/mL PEG propionate disulfide in HEPES buffer (10 mM HEPES, pH 7.4), and allowed to incubate overnight. The channels were then rinsed with purified water to leave behind films with biotin termination. After this, the channels were again filled with a 0.1 M $AgNO_3$ solution and another strip of silver was patterned downstream from the first one. The channels were rinsed and incubated with a solution containing DNP−PEG disulfide and 10 mg/mL PEG propionate disulfide in HEPES buffer for 30 min. Finally, the channels were rinsed and incubated with a 1 mg/mL solution of bovine serum albumin in PBS buffer (10 mM PBS, pH 7.2, $I = 150$ mM with NaCl) to block nonspecific adsorption of the analyte proteins.

After rinsing all three channels with buffer, various protein solutions were injected into each channel: (1) 0.1 mg/mL strep-A594 in PBS buffer, (2) a mixture of 0.1 mg/mL strep-A594 and 0.1 mg/mL of anti-DNP-A488 in PBS buffer, and (3) 0.1 mg/mL anti-DNP-A488 in PBS buffer. After 20 min of incubation, the channels were rinsed for a final time with PBS buffer and fluorescence images were obtained with both a green and red filter set. The combined false color image is shown in Figure 4. The image clearly demonstrates that the streptavidin (labeled red) binds almost exclusively to regions within the channel where the Ag nanoparticle film has been functionalized with biotin, while

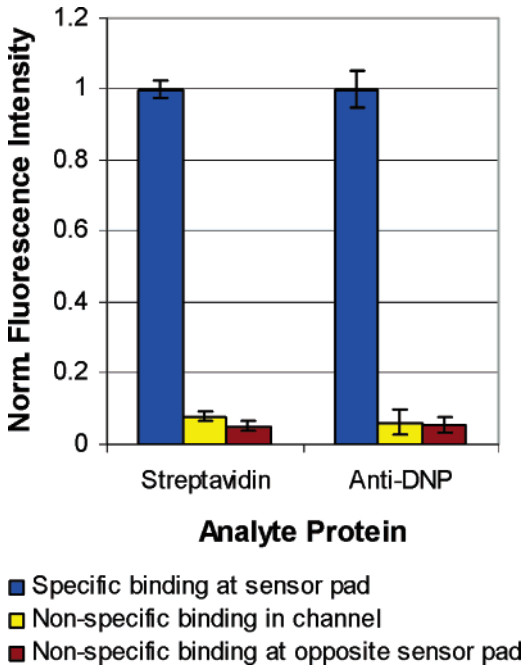

Figure 5. Bar graph of the normalized fluorescence intensity of analyte proteins binding specifically to their respective sensor pads (blue), analyte nonspecifically binding in the channel floor (yellow), and nonspecific adsorption at the opposite sensor pad (brown).

the anti-DNP antibody (labeled green) binds overwhelmingly at regions within the channel where the DNP was presented.

The data in channel 2 demonstrate the binding of both proteins from the same solution to different locations with good selectivity, illustrating the possible multiplexing and combinatorial potential for this technique. Figure 5 shows the normalized fluorescence intensity of the specifically bound proteins (blue) compared to the background signal from nonspecific interactions in the middle of the channel (yellow) as well as the nonspecific interactions at the sensor pad presenting the opposite ligand (brown). In all cases, the specific binding of analyte proteins was between 1 and 2 orders of magnitude greater than nonspecific absorption.

These simple experiments illustrate the ability of this method to pattern unique chemistries such as small molecules and proteins inside sealed microfluidic channels at specific addresses. In this case, our postassembly patterning method is useful for avoiding the exposure of patterned organic ligands to the harsh bonding conditions (i.e., oxygen plasma treatment) of PDMS to the TiO_2 surface.

Patterning Other Metals. TiO_2 nanoparticles can be used for the reduction of a variety of metals.[21] Therefore, the technique developed above for patterning silver should be generally applicable. Figure 6 shows the direct write patterning of Pd (Figure 6). In this case, Pd was deposited from a solution of 0.01 M $PdCl_2$ in 0.3 M acetic acid with a 20-min UV exposure onto a TiO_2 surface supported by a 0.5-mm-thick Pyrex substrate. As with silver, the method appears to be highly robust and easily performed inside sealed microfluidic channels. We have also successfully repeated this work with Cu and Au, although the nanoparticle sizes were somewhat larger.

DISCUSSION

The writing of metal nanoparticle films could be exploited for a variety of applications inside sealed microfluidic devices, and

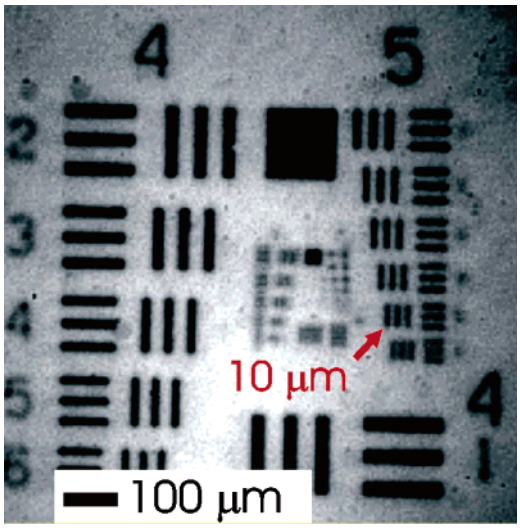

Figure 6. Bright-field image of Pd patterned onto TiO_2.

the technique is probably capable of near-diffraction-limited resolution. In the work presented herein, the resolution was somewhat limited by backside illumination. In other words, the backside contact mask procedure employed, in which light must transverse the thickness of the substrate, was the limiting factor rather than any inherent physical limit due to electron diffusion within the TiO_2 film. Using literature values for the electron diffusion coefficient in TiO_2, $D = 2.2 \times 10^{-5}$ cm^2/s,[32] as well as the electron−hole recombination lifetime, $\tau = 50$ ns,[33] it can be estimated in a simple two-dimensional random walk model, $L = (4Dt)^{1/2}$, that photogenerated electrons should diffuse only about a length, L, of 20 nm before recombining under the conditions we employ. The exact recombination lifetime depends on the intensity of the light used.[34] This calculation also assumes that the films are free of defects, and therefore, the actual travel distance may be even shorter for real films. Therefore, in the case of patterning with 365-nm light, the ultimate resolution should be close to 200 nm if high-quality projection optics were to be employed in the patterning procedure.

Using the methods described herein, it should be possible to rapidly screen the effects of Ag^+ concentration, temperature, and surfactant additives on metal nanoparticle size and geometry. This would be especially useful for particles deposited in pH, composition, or temperature gradients.[31,35] Furthermore, it should be possible to employ this lab-on-a-chip format for patterning not just individual metals but also for alloys, core shell structures,[36,37] and even gradient arrays of various metals. The use of microfluidics in this case offers the ability to rapidly optimize such deposition processes in a combinatorial manner. It could also allow for these materials to be exploited for high-throughput screening of catalytic properties, sensor development, and microreactor design.

(32) Kambe, S.; Nakade, S.; Wada, Y.; Kitamura, T.; Yanagida, S. *J. Mater. Chem.* **2002**, *12*, 723−728.
(33) Warman, J. M.; Dehaas, M. P.; Gratzel, M.; Infelta, P. P. *Nature* **1984**, *310*, 306−308.
(34) Colombo, D. P.; Bowman, R. M. *J. Phys. Chem.* **1995**, *99*, 11752−11756.
(35) Mao, H. B.; Yang, T. L.; Cremer, P. S. *J. Am. Chem. Soc.* **2002**, *124*, 4432−4435.
(36) Santra, A. K.; Yang, F.; Goodman, D. W. *Surf. Sci.* **2004**, *548*, 324−332.
(37) He, J. H.; Ichinose, I.; Kunitake, T.; Nakao, A.; Shiraishi, Y.; Toshima, N. *J. Am. Chem. Soc.* **2003**, *125*, 11034−11040.

Functionalizing nanoparticle films inside of microfluidic channels may offer new opportunities for biosensors or screening assays. The ability to address individual ligands atop nanoparticle films inside microfluidic devices could be combined with such technologies as transmission surface plasmon resonance spectroscopy[38−41] or surfaced-enhanced fluorescence.[42−44] This could allow for the development of powerful lab-on-a-chip devices with label-free detection or fluorescence detection with enhanced sensitivity.

Immobilizing patches of oriented enzymes inside microfluidic devices for enzymatic microreactors is another potential application of this technique. By binding enzymes linked to antibodies or streptavidin, one could spatially address arrays of enzymes inside microfluidic devices for the development of complex enzymatic microreactors. Such reactors could perform a series of chemical modifications to a substrate within a single channel. This process might even be multiplexed across several channels utilizing a variety of enzymes for combinatorial synthesis.

(38) Tokareva, I.; Minko, S.; Fendler, J. H.; Hutter, E. *J. Am. Chem. Soc.* **2004**, *126*, 15950−15951.
(39) Lahav, M.; Vaskevich, A.; Rubinstein, I. *Langmuir* **2004**, *20*, 7365−7367.
(40) Hutter, E.; Pileni, M. P. *J. Phys. Chem. B* **2003**, *107*, 6497−6499.
(41) Kalyuzhny, G.; Schneeweiss, M. A.; Shanzer, A.; Vaskevich, A.; Rubinstein, I. *J. Am. Chem. Soc.* **2001**, *123*, 3177−3178.
(42) Geddes, C. D.; Parfenov, A.; Roll, D.; Fang, J. Y.; Lakowicz, J. R. *Langmuir* **2003**, *19*, 6236−6241.
(43) Sokolov, K.; Chumanov, G.; Cotton, T. M. *Anal. Chem.* **1998**, *70*, 3898−3905.
(44) Attridge, J. W.; Daniels, P. B.; Deacon, J. K.; Robinson, G. A.; Davidson, G. P. *Biosens. Bioelectron.* **1991**, *6*, 201−214.

ACKNOWLEDGMENT

We thank the Army Research Office (W911NF-05-1-0494) and the National Institutes of Health (GM070622) for funding. P.S.C. also acknowledges additional fellowship support from a Beckman Young Investigator Award, an Alfred P. Sloan Research Fellowship, and a Camille Dreyfus Teacher-Scholar Award. We also thank Dr. Tinglu Yang, J. Garrott Slaton, and Richard J. Duffy for useful discussions.

Received for review July 20, 2005. Accepted October 18, 2005.

AC051288J